



A support system for civil aviation navigation equipment security management

Quan Shao^{a,*}, Meng Jia^a, Chenchen Xu^b, Xiaojia Feng^c

^a College of Civil Aviation, Nanjing University of Aeronautics and Astronautics, Nanjing, China

^b Social and Economic Geography Group, Department of Geography, Ghent University, Ghent, Belgium

^c China Eastern Airlines Jiangsu Limited, Nanjing, China

ARTICLE INFO

Keywords:

Civil aviation safety
Navigation equipment system
Sustainability assessment
Equipment expansion planning

ABSTRACT

Civil aviation navigation equipment system has many weaknesses, which easily causes serious problem to air transportation safety. This paper focuses on a support system for civil aviation navigation equipment security management. Firstly, a sustainability assessment platform was constructed to analysis and find out the weaknesses of equipment network. Next, one network expansion planning platform was built to improve the reliability and business continuity of the whole navigation system. Experiments were carried out based on these two platforms. Also, the equipment network of China's eastern part was expanded based on the business continuity assessment. Results proved that the network business continuity and node efficiencies of new equipment network can satisfy the lowest requirement of economic consumption. Finally, the optimal network expansion planning method has been achieved, proving the effectiveness of the civil aviation navigation equipment security management support system.

1. Introduction

With the flourishing development of civil aviation and the ever-increasing air traffic flow, higher requirement to civil aviation security management has been raised in recent years. However, frequent natural disasters have brought tremendous pressure to Air Traffic Control (ATC) security systems and also has exposed the vulnerability of ATC system. ATC security equipment interrelates and cooperates with each other. Single equipment failure may cause chain effect and lead to large-area ATC business paralysis. Therefore, a civil aviation navigation equipment security management system is in great need to perform sustainability assessment and expansion of ATC security equipment.

According to the definition given by NavyBMR ([Aviation Support Equipment](#)), aviation support equipment is all equipment required on the ground to make an aeronautical system, system command and control system, support system, subsystem, or end item of equipment operational in its intended environment. This paper focused on the aviation navigators on ground, which are essential to make sure the security of flight security. Many scholars have devoted to conducting researches on civil aviation security systems in order to promote the whole system reliability, stability and business continuity. Existing studies focused on civil aviation security risk management from several aspects, including ATC crew, ATC equipment, environment, and

management. By establishing an assessment index system, the potentially dangerous sources in the operation of ATC equipment could be identified and evaluated. Then, corresponding measures can be adopted to reduce the risk to a tolerable range ([Kontogiannis and Malakis, 2009](#); [Prandini et al., 2011](#); [Chen et al., 2013](#)), which is the acceptable risk level range in air traffic control. In accordance with the safety management regulations of International Civil Aviation Organization (ICAO), a safety management system of ATC system will be meaningful to control and eliminate potential dangerous ([Besada et al., 2016](#); [Wang, 2014](#); [Gravio et al., 2015](#)). These studies paid close attention on self-assessment but a unified and strict third-party assessment index system is still the missing part. Moreover, there have been some studies which analyzed the reliability and stability of ATC equipment. These methods can be used to evaluate the network characteristic and business continuity of the security system in various scenarios, including multi-constraint air traffic control equipment layout planning algorithm based on complex network ([Shao et al., 2012](#)), toll-pulling force detection device of ATC system ([Li et al., 2015](#)), fuzzy petri net model to evaluate aircraft guarantee system ([Feng et al., 2010](#)), and many air traffic control system quantitative evaluation framework ([Liu et al., 2016](#); [Tikhvinskiy et al., 2017](#); [Schnell et al., 2014](#); [Subotic et al., 2014](#); [Li et al., 2017](#)). Recently, some new studies have been proposed to search for better way to improve aviation security. These studies

* Corresponding author.

E-mail address: shaoquan@nuaa.edu.cn (Q. Shao).

<https://doi.org/10.1016/j.ssci.2019.104578>

Received 11 October 2019; Received in revised form 18 November 2019; Accepted 11 December 2019

Available online 23 December 2019

0925-7535/ © 2019 Elsevier Ltd. All rights reserved.

concern about human factors (Filippov et al., 2019), aviation policy (Poghosyan, 2018), and Information Database Management System (Li et al., 2019). There are not many researches notices the function of a navigation system.

The above studies mainly focus on the reliability and location planning of single ATC equipment, but they are lack of systematic analysis of ATC security equipment coordinated operation, such as equipment coverage range, operating environment and influence of location on security capability. At the same time, the cost of establishing navigation stations has been ignored sometimes. Civil aviation security equipment network is a weighted topological network, which regards equipment set as nodes, air routes as edges, and security capabilities as weights. In other words, the connection preference of civil aviation security equipment is similar to self-organization characteristic of lifeline networks. Similarly, many other important equipment systems, such as the gas pipe networks (Shimizu et al., 2006), power networks (Jacob and Hari Krishnan, 2018; Hejeejo, 2017) and water supply networks (Karsten et al., 2015), in city lifeline engineering, also face the problems of equipment security planning and cascading failure vulnerability. Like many other cases, the constitutive property, connectivity, and functionality of the network are closely related to the equipment security planning. Therefore, aviation security equipment network is a whole network framework with air routes at the edge, and it is of great significance to establish a civil aviation navigation equipment safety support system to realize the holistic safety management function.

Civil aviation equipment network has navigation station strongholds as nodes. There is a border right with the weight of the reliability guaranteed by the equipment. However, aviation equipment network is the framework with the air route guaranteed by the equipment as the side. To improve the operation of air traffic control, this paper constructed a support system for civil aviation navigation equipment security management. In this system, the network topology of civil aviation support equipment and the weighted network model with the weight of flight flow are constructed to study and analyze the service continuity. From two aspects of network structure and network function, the node efficiency can be theoretically supported. The equipment network sustainability assessment model, and finally consider the factors of signal coverage, construction cost and network stability to construct a new equipment location planning model. Particularly, the sustainability assessment is useful for evaluating the security level of existing civil aviation navigation station networks. And network expansion can be conducive to ensure the security level of network service in case of growing air traffic flow.

2. Method

To set up this sustainability assessment platform, an aviation security equipment system was first constructed to be the basis for further calculation in complex networks. Next, to assess aviation navigation equipment sustainability, the node vulnerability assessment method was proposed based on network topology, and a node service sustainability assessment method was proposed based on network function. Finally, to realize the navigation equipment extension planning, this paper analyzed the navigation equipment signal coverage range and modeled the navigation station location.

2.1. Aviation security equipment system construction

2.1.1. Construction of weighted network

According to the relations between the aviation security equipment network and the air route network, weighted network model was established based on air route network with security capacities of radar and very high frequency (VHF) communication equipment as weight. Thus, this paper chose navigation stations as nodes, air routes which connect these navigation stations as edges, and security capacities of

radar and VHF equipment as edge weight to construct the network model. The aviation security equipment network model was shown as Eq. (1).

$$G = (V, E, A, K_1, K_2) \quad (1)$$

In which, n is the number of nodes in network. $V = (v_1, v_2, \dots, v_n)$ means node set of navigation stations, $E = (e_1, e_2, \dots, e_m)$ represents edge

set of air routes, and $A_{n \times n} = \begin{bmatrix} 1 & \delta_{12} & \dots & \delta_{1n} \\ \delta_{21} & 1 & \dots & \delta_{2n} \\ \vdots & \vdots & \ddots & \vdots \\ \delta_{n1} & \delta_{n2} & \dots & 1 \end{bmatrix}$ is an adjacent matrix which

represents relations among nodes in network. In addition, $\delta_{ij} = 0$ denotes no physical relations between two nodes. By contrast, $\delta_{ij} = 1$ denotes that these two nodes are connected by a physical relation.

$K_1 = \{k'_{ij} > 0 \mid i, j = 1, 2, \dots, m\}$ is a value set of the radar security capacity as weight between node i and j . Security capacity refers to the largest air traffic flow which can be safely serviced by certain navigation stations.

$K_2 = \{k'_{ij} > 0 \mid i, j = 1, 2, \dots, m\}$ is value set of VHF security capacity as weight between node i and j .

Q is defined as security weight of civil aviation security equipment network, which is the sum of radar weights and VHF weights on air routes. Q is described as Eq. (2).

$$Q = K_1 \times K_2 \quad (2)$$

Then, civil aviation security system network model is described as Eq. (3).

$$G = (V, E, A, Q) \quad (3)$$

Generally, some differences in interaction strength exist among different navigation stations. Airspace flow, as a direct exchange among navigation stations, visually illustrates interaction strength among pairs of navigation stations. Navigation station tolerability reflects its operational capacity and determines flight flow. Thus, construct a weighted network model with flight flow as edge weight to describe interaction strength among pairs of navigation stations.

Assuming there are n navigation station nodes and m air routes. Flight flow k_{ij} is regarded as the edge weight among navigation station i and j . Flow between each pair of navigation stations is an undirected scalar, which means $k_{ij} = k_{ji}$. Thus, the equipment security weighted network is defined as Eq. (4).

$$G = (V, E, A, Q, K) \quad (4)$$

$K = \{k_{ij} > 0 \mid i, j = 1, 2, \dots, m\}$ is the set of values for the flow as weight between node i and node j . Flow weight is a network function value with actual physical significance and ignoring structure characteristics. It not only reflects the actual importance of air routes and interaction strength among navigation stations but also measures the importance of communication and surveillance equipment. If security weight is great and flow weight is small, equipment redundancy will be high and causes equipment waste. By contrast, if security weight is small and flow weight is great, business service will be discontinuous. Thus, only security weight and flow weight bring out the best in each other can maximize the utilization of equipment. Equipment location is planned base on the using of minimum equipment to ensure the maximum flow.

Equipment security importance is proposed as Eq. (5) to reflect relations between security weights and load weights.

$$Im_{ij} = \frac{K_{ij}}{Q_{ij}} \quad (5)$$

The lower Im_{ij} reveals higher security weight and lower flow weight. That is equipment redundancy. The higher Im_{ij} reveals lower security weight and higher flow weight. That means equipment is more important and fragile.

Besides, define the interaction strength of each navigation station as

the sum of flight flow of air routes that consisted of all adjacent navigation stations connecting with this navigation station. It is represented as Eq. (6).

$$D_i = \sum_{j \neq i} k_{ij} \quad (6)$$

Then, construct the following equipment security weighted topology network according to the Jeppesen chart of Guiyang airport terminal and airspace flow distribution.

2.1.2. Flow weight and node strength distribution

In aviation equipment security network, flow weights are similarity weights based on the definition of similarity weight in literature (Zhou et al., 2012). That means weight is in inverse proportion to distance. Thus, $d_{ij} = 1/k_{ij}$. Regard per segment of air route as one unit. d_{ij} denotes the shortest distance between navigation station i and j , which is the least number of segments.

Some probability distributions exist in each air route flight flow in accordance with market requirement in civil aviation actual operation, that is $k_{ij} \sim \rho(\omega)$. Airspace flow statistics of Southwest China in 2014 from Southwest Regional Air Traffic Management Bureau of Civil Aviation of China are counted in the light of each navigation station in Fig. 1. This paper treated the total flow of one navigation station as its flow weight, and used the proportion of each navigation station to represent the flow weight distribution of equipment. Edges in network structure are endowed with weights in the form of percentages. Detail data is displayed in Table 1.

The flow weight distribution is shown in Fig. 2 according to the statistics data in Table 1. Node strength distribution is calculated according to flow weight distribution (Eq. (5)) and interaction strength of navigation stations (Eq. (6)), which is shown as Fig. 3.

The tendencies of lines in Fig. 2 and Fig. 3 follow the power-law distribution and verify the scale-free properties of civil aviation equipment security network. Meanwhile, only a few nodes (the navigation station P_3 , P_2 and P_5) and edges (the air route $k_{3,2}$, $k_{3,5}$ and $k_{3,12}$) carry the lifeblood of the whole network. However, these nodes and edges, as the critical points of equipment network, are weaknesses in the network and can be regarded as alternative areas of location planning.

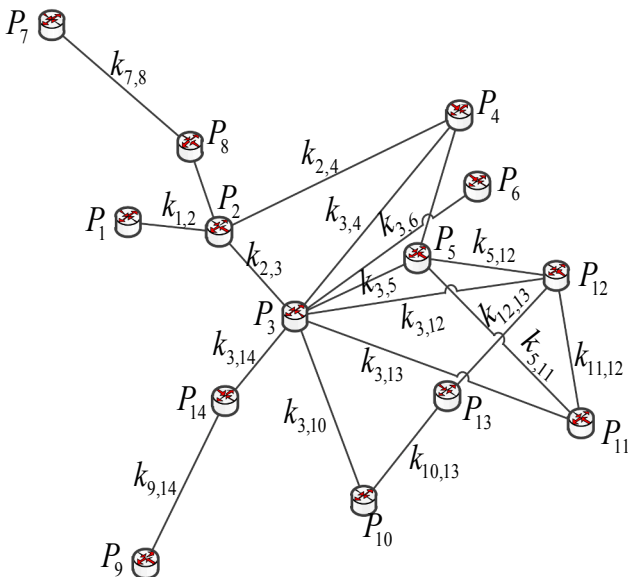


Fig. 1. Equipment security weighted topology network of Guiyang airport terminal.

2.2. Aviation navigation equipment sustainability assessment

2.2.1. Node vulnerability assessment based on network topology

If some navigation stations are failure in actual ATC equipment security system, flight courses via these navigation stations will change, then flight flow of the whole network will be reassigned. Thus, the flight flow of fault navigation stations is assigned to their adjacent navigation stations. If the adjacent navigation stations can bear the new assigned flight flow, network will still operate fluently. Otherwise, if the flow of adjacent navigation stations exceeds their limit load, it denotes improper flow assignment and needs further flow assignment. Thus, node vulnerability is closely related to node location and its adjacent node contribution.

Node efficiency is introduced to combine node overall vulnerability with adjacent node contribution. In this paper, node efficiency refers to the difficulty for information to extent from this navigation station to other navigation stations, which reflects navigation station control ability to network flight flow. Node efficiency is defined as Eq. (7).

$$I_i = \frac{1}{n-1} \sum_{j=1, j \neq i}^n \frac{1}{d_{ij}} \quad (7)$$

The larger node efficiency value means that the more important node is in network flow transmitting procedure and the more likely network vulnerability increases when suffers from attack. That is because when the device network is attacked in a certain way, the failed navigation station will cause the air traffic transmission pattern and other navigation station traffic load changes. And once the navigation station load exceeds the limit load, the navigation platform will be invalidated, and in turn affect other navigation. Conversely, the smaller the node efficiency value, the fewer failed navigation stations will appear if the network is hit.

Vulnerability contribution topology relations among pairs of navigation stations are developed because of vulnerability transfer in the connection of navigation stations. This is a map of actual network topology. The main vulnerability contribution relations are reflected among adjacent navigation stations, which can be described in an adjacent matrix. So, vulnerability contribution relation among navigation stations is shown as Eq. (8).

$$F_c = \begin{bmatrix} 1 & \delta_{12}D_2/(l)^2 & \dots & \delta_{1n}D_n/(l)^2 \\ \delta_{21}D_1/(l)^2 & 1 & \dots & \delta_{2n}D_n/(l)^2 \\ \vdots & \vdots & \ddots & \vdots \\ \delta_{n1}D_1/(l)^2 & \delta_{n2}D_2/(l)^2 & \dots & 1 \end{bmatrix} \quad (8)$$

In which, n is the number of nodes. l is network average degree value. D_i is degree value of node i . δ_{ij} is an element in adjacent matrix. If navigation station i and j are connected, $\delta_{ij} = 1$. Otherwise, $\delta_{ij} = 0$. $D_i/(l)^2$ denotes node i 's importance degree contribution to each adjacent node. It is observed from Eq. (8) that node importance degree is assigned to adjacent nodes equally. But in an actual physical situation, aircraft must select suitable and shortest navigation stations under the limiting condition of fuel quantity, aircraft type, and driver license when aircraft changes route or flies to alternative airports due to some navigation stations failure. Hence, vulnerability contribution matrix F_c is amended as follows fused with node efficiency.

$$\text{Correction 1. } F_r = F_c \times \begin{pmatrix} I_1 & 0 & \dots & 0 \\ 0 & I_2 & \dots & 0 \\ \vdots & \vdots & \ddots & \vdots \\ 0 & \dots & 0 & I_n \end{pmatrix}. \text{ As shown in Eq. (9), degree de-}$$

notes node local importance. Node efficiency denotes overall importance in the whole network. Thus, node importance value contributed to adjacent nodes is exactly expressed by multiplying itself node efficiency.

Table 1

Flow weight distribution of equipment security weighted network.

Edge	Weight (%)	Edge	Weight (%)	Edge	Weight (%)	Edge	Weight (%)
$k_{3,2}$	15.36	$k_{2,4}$	6.47	$k_{13,12}$	3.14	$k_{9,14}$	2.82
$k_{3,5}$	9.97	$k_{2,8}$	5.76	$k_{3,14}$	3.18	$k_{1,2}$	2.66
$k_{3,12}$	9.41	$k_{5,12}$	5.42	$k_{3,4}$	2.93	$k_{7,8}$	2.47
$k_{3,10}$	6.97	$k_{3,11}$	4.55	$k_{5,11}$	2.91	$k_{3,6}$	2.42
$k_{4,5}$	6.69	$k_{13,10}$	3.72	$k_{11,12}$	2.9	—	—

$$F_r = \begin{bmatrix} I_1 \delta_{12} D_2 I_2 / (I)^2 \cdots \delta_{1n} D_n I_n / (I)^2 \\ \delta_{21} D_1 I_1 / (I)^2 I_2 \cdots \delta_{2n} D_n I_n / (I)^2 \\ \vdots \vdots \vdots \\ \delta_{n1} D_1 I_1 / (I)^2 \delta_{n2} D_2 I_2 / (I)^2 \cdots I_n \end{bmatrix} \quad (9)$$

Some differences consist in importance degree of the whole network due to various node efficiencies in each adjacent navigation station in actual physical situation. That is, node contribution values are assigned to each adjacent node according to different ratios. The higher efficiencies of adjacent navigation stations are, the better connectivity of this station is, and also the shorter distance to other stations is. Thus, contribution value is easier to be assigned to the adjacent stations whose efficiencies are higher when navigation station fails. The distribution proportions of contribution values are determined by efficiencies of adjacent nodes and total efficiency of all nodes in network.

$$\text{Correction } 2.F_v = \begin{pmatrix} I_1 & 0 & \cdots & 0 \\ 0 & I_2 & \cdots & 0 \\ \vdots & \vdots & \ddots & \vdots \\ 0 & 0 & \cdots & I_n \end{pmatrix} \times F_{r(n \times n)} \text{ is brought in Eq. (10).}$$

$$F_v = \begin{bmatrix} I_1^2 \delta_{12} D_2 I_2 / (I)^2 \cdots \delta_{1n} D_n I_n / (I)^2 \\ \delta_{21} D_1 I_1 / (I)^2 I_2^2 \cdots \delta_{2n} D_n I_n / (I)^2 \\ \vdots \vdots \vdots \\ \delta_{n1} D_1 I_1 / (I)^2 \delta_{n2} D_2 I_2 / (I)^2 \cdots I_n^2 \end{bmatrix} \quad (10)$$

Then, navigation station vulnerability assessment model is proposed in comprehensive consideration of overall vulnerability of this station I_i and vulnerability contribution of adjacent stations $\sum_{j=1, j \neq i}^n \delta_{ij} D_j I_j I_i / (I)^2$, which is shown as Eq. (11).

$$W_i = I_i + \sum_{j=1, j \neq i}^n \delta_{ij} D_j I_j I_i / (I)^2 \quad (11)$$

2.2.2. Node service sustainability assessment based on network function

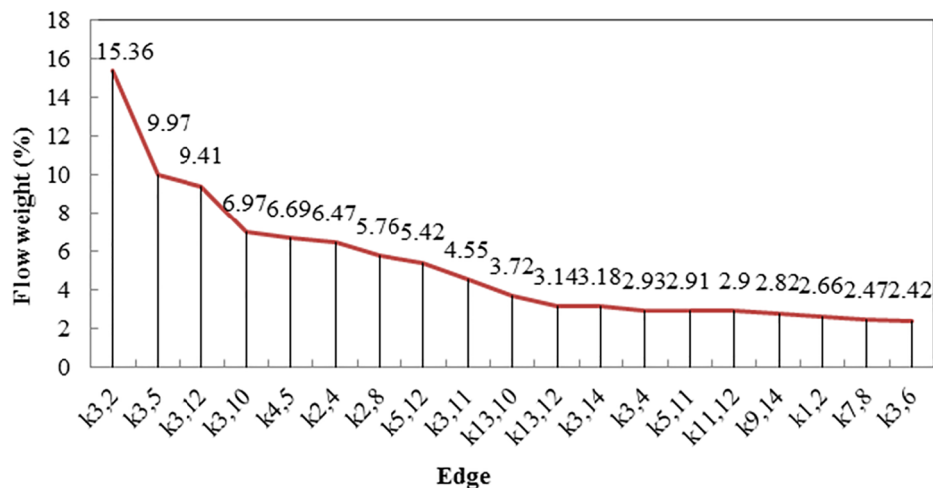
Business continuity refers to the adoption of appropriate technical means to identify the critical role of key units by identifying the key elements of the system and the sources of danger that may pose a threat to key units. Business continuity management is a holistic management process that provides a framework for building rapid recovery and effective response capabilities by identifying potential hazards, thereby reducing the impact of disasters on the business. Node service sustainability is the business continuity of navigation station in the networks.

Node efficiency reflects load on itself to some extent because the sum of all node efficiencies is network efficiency (Dai and Wan, 2014). In ATC equipment security system, the higher node efficiency is, the shorter distance to other navigation stations is. This indirectly reflects the bigger network business continuity of navigation station is, the bigger load this station bears. Thus, node load is represented by node efficiency, which is defined as Eq. (12).

$$L_i = \exp(\lambda I_i) \quad (12)$$

In which, λ denotes relations between node efficiency and node load, and $\lambda > 1$.

The main ATC navigation equipment is very high frequency omnidirectional range (VOR)/ distance measuring equipment (DME) at present. A certain flight interval among airplanes should exist to ensure safety flight due to influences of navigation station working frequency, capacity, and range, as well as an accurate degree in usage. Thus, the navigation station's load saturation C_0 is determined by the minimum interval among airplanes. The flow of redundant airplanes will be controlled if the number of navigated airplanes exceeds navigation station load saturation. Usually, the number of channels on navigation station working frequency is limited, and flight flow is increasing. Flow control is needed within a tolerable range to maximize the utilization of each navigation station. Its upper limit of load is defined as limit load. Assuming load saturations of each navigation station are the same. Three loads are configured to each station node, which are ideal load,

**Fig. 2.** Flow weight distribution diagram of equipment security weighted network.

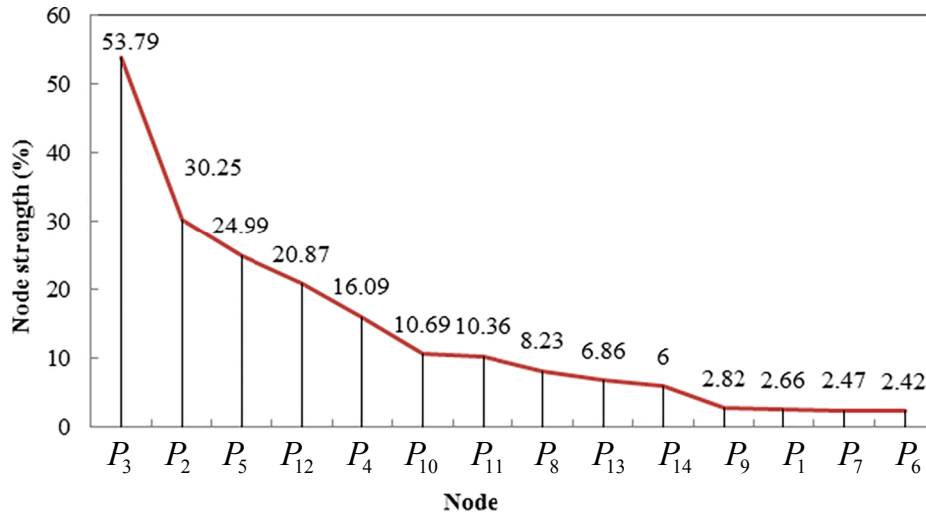


Fig. 3. Node strength distributions of equipment network.

tolerable load and limit load.

In detail, ideal load is the load that node load is less than or equal to load saturation, $L_i \leq C_0$. Tolerable load is the load that control flow within a tolerable range, $C_0 < L_i < \alpha C_0$, $\alpha \geq 1$. Limit load describes flight flow exceed the tolerable range, $C_\infty = \alpha C_0$.

Failure probability exists in navigation station when it suffers from flight flow control according to navigation station load. This failure is caused by discontinuity of business service but not failure of equipment itself. Failure probability model is constructed as Eq. (13).

$$p_i = \begin{cases} 1 & L_i \leq C_0 \\ \frac{\alpha C_0 \cdot \exp(-\lambda L_i)}{\exp(\lambda L_i) \times (\alpha - 1)} & C_0 < L_i < \alpha C_0 \\ 0 & L_i \geq \alpha C_0 \end{cases} \quad (13)$$

$p_i = 1$ denotes ideal load (navigation station load is within the range of load saturation).

$p_i = 0$ denotes navigation station load exceeds limit load. This is an unrealistic existence because navigation station load is close unlimitedly to limit load with gradually increasing tendency but it is unable to reach limit load.

When the equipment network suffers from some attack, the fault navigation station will cause the change of the spatial flow transfer pattern. Once navigation station load exceeds limit load, it will lead to navigation station failure and further influence flow load of other navigation stations. The fewer the number of failure navigation stations is, the stronger the normal working ability of equipment security system is under the condition of suffering from attack.

2.3. Navigation equipment extension planning

2.3.1. Navigation equipment signal coverage range analysis

The maximum operating distance of VOR is confirmed as Eq. (14) according to its working principle without regard to reflect, refraction and absorption of landform and space radio wave.

$$R_{\max} = \frac{\sqrt{30P_t G'}}{E_e} \times 1000 \quad (14)$$

In which, R_{\max} is the maximum operating distance of VOR in free space. P_t is average power at output port of transmitter. G' is antenna gain. E_e is electric field intensity at signal receiver point.

The Shielded angle of equipment is calculated from all directions in order to obtain equipment actual operating distances. Computational formula of shielded angle is shown as Eq. (15).

$$\theta_s = \frac{h_s - h_a}{17.45d_s} - \frac{d_s}{296.5} \quad (15)$$

In which, h_s - aircraft's flight height, h_a - the height of the navigation station's antenna, d_s - the distance from obstacle to navigation station.

In practical application, we add a correction factor.

$$\theta_{rs} = \theta_s + 3.16\sqrt{\lambda_0/d_i} \quad (16)$$

In which, λ_0 - working wavelength of navigation station, d_i - corresponding obstacle slant range of shielded angle.

Then, equipment coverage distance from various directions in calculated as Eq. (17) using shielded angles.

$$R_s = \sqrt{(R_e + \tan \theta_{rs})^2 + 2R_e(h_s - h_a)} - R_e \tan \theta_{rs} \quad (17)$$

In which, $R_e = 4R_0/3$ - equivalent earth radius, R_0 - actual earth radius.

Therefore, we can obtain the actual coverage range of equipment signal according to signal transmission distance in free space, sight cut-off distance and digital geographical elevation data. Calculating equipment's actual operating distance helps to avoid the existence of a signal dead zone during equipment planning and realize signal multiply coverage.

2.3.2. Construction of the model for navigation station location

Optimize the navigation station location based on requirement of wireless environment, which not only enhance reliability and stability of navigation system but also minimum investment and cost. This paper introduces node efficiency to reduce calculation amount in one large-scale network by using network business continuity to plan navigation station location (Feng et al., 2010). Established Objective function in the consideration of low establishment cost, balanced air route business continuity and balanced node efficiency.

(1). Objective function based on network structure

This objective function corresponds to the largest air route business continuity variance and efficiency variance value of the navigation station node in the new network after adding new navigation stations. It minimizes the differences in the average values of the air route business continuity and node efficiency between new network and old network. In the condition of guaranteeing the normal operation of network, the distribution of network security capacity is balanced and critical indexes of edges and nodes are decreased. Meanwhile, network security capacity and reliability are correspondingly improved. Since orders of magnitude of air route business continuity and navigation station node

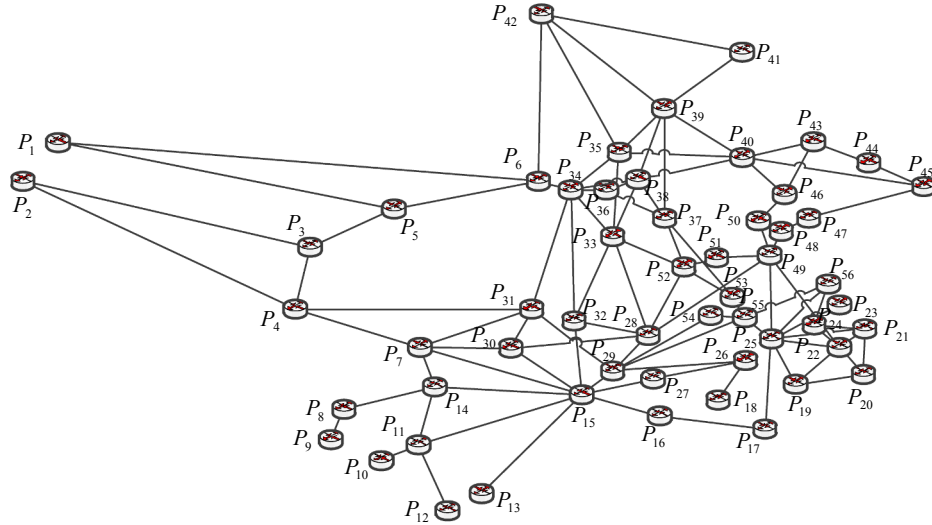


Fig. 4. Network topological graph of China southeast area.

efficiency are not the same, the objective function is described as Eq. (18) and Eq. (19).

$$L(M_i) = \begin{cases} \min(\mu'_l - \mu_l) \\ \max(\sigma_l^2 - \sigma_l'^2) \end{cases} \quad (18)$$

$$P_v(M_i) = \begin{cases} \min(\mu'_p - \mu_p) \\ \max(\sigma_p^2 - \sigma_p'^2) \end{cases} \quad (19)$$

In which, μ_l and μ_p are respectively average values of air route edge business continuity and navigation station node efficiency in original network. μ'_l and μ'_p are respectively average values of air route edge business continuity and navigation station node efficiency in new network after adding new navigation stations. σ_l^2 and σ_p^2 are respectively variances of air route edge business continuity set and navigation station node efficiency set in original network. $\sigma_l'^2$ and $\sigma_p'^2$ are respectively variances of air route edge business continuity set and navigation station node efficiency set in new network after adding new navigation stations.

Two constraint conditions are proposed in this paper.

① New air routes must satisfy the maximum operating distance of VOR.

$$S(l'_i) \leq R_{Max} \quad (20)$$

In which, $S(l'_i)$ is distance between any two navigation stations. R_{Max} is the maximum operating distance of navigation station based on shielded angle.

② Distance from new navigation station to high efficient navigation station should be less than the maximum operating range of VOR.

$$D_{vor}^p \leq R_{Max} \quad (21)$$

In which, D_{vor}^p is distance from alternative navigation station to high efficient navigation station.

(2). Objective function based on establishment cost

Navigation station establishment cost covers equipment original pricea, land expropriation costb, construction feeec, site formation feed, process installation and supporting facilities fee, project management feef, survey and design feeg, and operating maintenance feeht.

Variables from 0 to 1 are introduced to select location plan. M_i is plan i . If plan i is selected, $M_i = 1$. Otherwise, $M_i = 0$. Then, objective function is constructed as Eq. (22).

$$\min z(M_i) = aM_i + bM_i + cM_i + dM_i + eM_i + fM_i + gM_i + hM_i \quad (22)$$

Constraint conditions are shown as Eq. (23) and Eq. (24).

$$M_1 + M_2 + M_3 + \dots + M_n = 1 \quad (23)$$

$$M_i = \begin{cases} 1, & \text{plan is selected} \\ 0, & \text{plan is not selected} \end{cases} \quad (24)$$

Through comprehensive consideration of the weights of network business continuity and establishment cost, the multi-objective programming is further constructed to optimize navigation station location. Objective function of multi-objective programming is shown as Eq. (25).

$$\min C(M_i) = k_1 z(M_i) + k_2 L(M_i) + k_3 P_v(M_i) \quad (25)$$

Then, constraint conditions are constructed as Eq. (26) to Eq. (29).

$$S(l'_i) \leq R_{Max} \quad (26)$$

$$D_{vor}^p \leq R_{Max} \quad (27)$$

$$M_1 + M_2 + M_3 + \dots + M_n = 1 \quad (28)$$

$$M_i = \begin{cases} 1, & \text{plan is selected} \\ 0, & \text{plan is not selected} \end{cases} \quad (29)$$

3. Results and discussion

3.1. Analysis of node vulnerability

Civil aviation equipment security weighted network was constructed by taking China southeast area as an example based on the above function expression. The network topological graph of China southeast area is shown as Fig. 4.

Fig. 4. Network topological graph of China southeast area.

There are 56 nodes in equipment network in China southeast area. Two nodes are selected discretionarily from these 56 nodes to calculate the shortest distance among nodes, which is regarded as a segment. Then, the shortest distance among nodes is taken to node efficiency formula Eq. (7) to obtain efficiency values of each node. The adjacent node contribution is determined by calculating degree value. The following three-dimensional scatter chart, which is shown in Fig. 5 is drawn based on Mathematica software, which is regarded node efficiency as X-axis, adjacent node contribution as Y-axis and node vulnerability as Z-axis.

Since these dots discretely distribute in three-dimensional space,

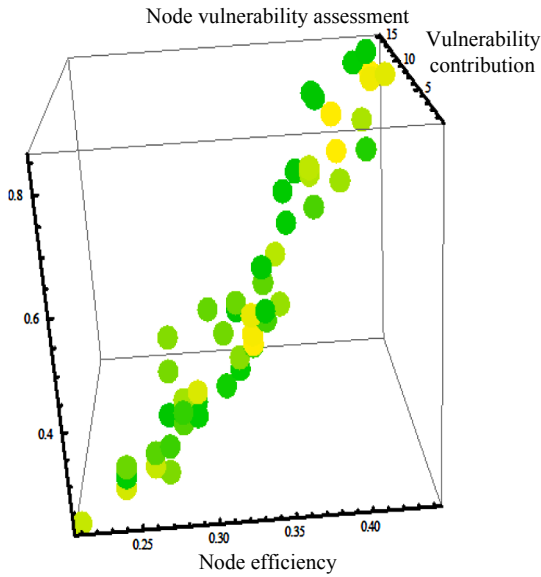


Fig. 5. Three-dimensional simulation scatter chart of node vulnerability assessment.

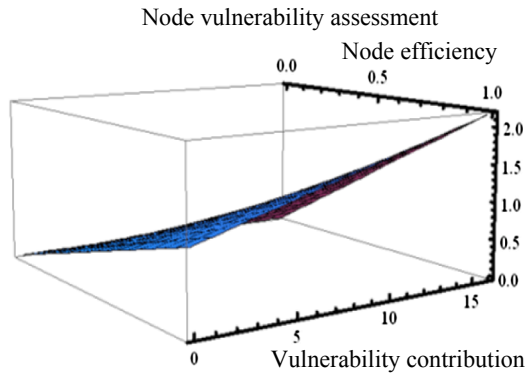


Fig. 6. Three-dimensional surface fitting chart of node vulnerability assessment.

they are mounted to a continuous three-dimensional surface to perceive exact coordinates. Place the dots and surface in the same coordinate system to observe visually the relations of node efficiency and adjacent node contribution to node vulnerability, which is shown in Fig. 6.

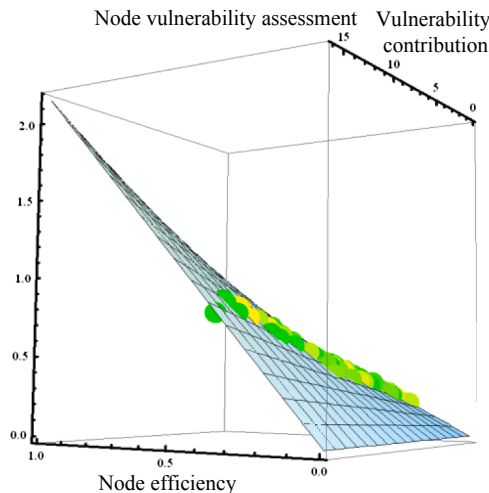


Fig. 7. Node vulnerability assessment attached on three-dimensional fitting surface.

Results in Fig. 7 show the discrete node vulnerability still follows the power-law distribution and only a few node vulnerability values are larger at the top of assessment model. The vulnerability of navigation station is the biggest at P_{34} (0.85), closely followed by P_{15} and P_{28} (0.82). These nodes, as the critical links in network, maintain the lifeline of the whole network. Meanwhile, unbalanced distribution of network vulnerability is scattered from 0.26 to 0.85. Most nodes have poor connectivity and a certain redundancy. Thus, optimize the network layout by adding equipment and increasing air routes.

3.2. Analysis of node failure

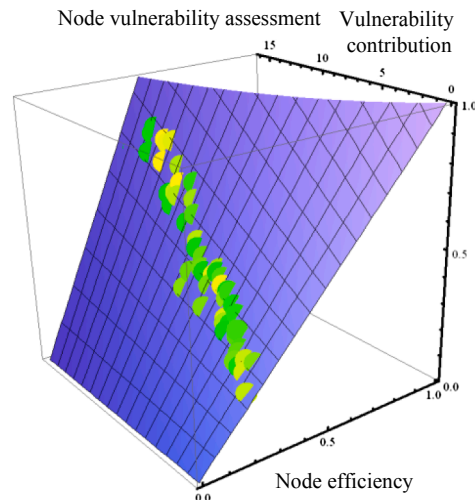
Some differences exist in the capacity saturation and tolerance of each navigation station due to influences of equipment types and external factors in actual physical situation. Two controls, a and $Global\backslash C$, respectively represents tolerance and capacity saturation. Influences of tolerance load and limit load on node business continuity are observed by adjusting and controlling coefficients of a and $Global\backslash C$. $\lambda = 10$. The value ranges of tolerance a and capacity saturation C_0 are random ranges satisfying constraint conditions for theoretically verifying assessment model but they cannot really reflect the actual tolerance and capacity saturation of civil aviation navigation stations. The simulation was conducted from the two aspects of considering node tolerance and without considering node tolerance. The value ranges of $Global\backslash C$ and a are respectively set from 1 to 8 and from 1 to 20. The simulation results are shown in Fig. 8 and Fig. 9.

In Fig. 8, $a = 1$ when tolerance is not taken into consideration. Besides, $Global\backslash C$ is adjusted to 2.19 and 6.69 respectively.

Results reveal that airspace flow exceeding the maximum capacity of navigation station is considered that navigation station cannot ensure security continuity, when there is no tolerance in navigation station (that is no redundancy of flow control). Thus, airspace flow may be ensured only by adding capacity saturation of each navigation station to satisfy the continuous increase of airspace flow. This means that technical content of each equipment should improve to enhance security capacity (capacity saturation) of navigation stations.

In Fig. 9, node saturation $Global\backslash C$ is always set as 3.31 in the consideration of navigation station tolerance. Navigation station tolerance a is adjusted to 6.5 and 18.5 respectively.

Results reveal the decline of node security probability is more easing with the increase of navigation station tolerance under the acceptable flow control when taken node toleration into consideration. The increases of each navigation station flow load upper limit means navigation station capacity saturation is virtually increased by some flow control in a constant equipment security capacity.



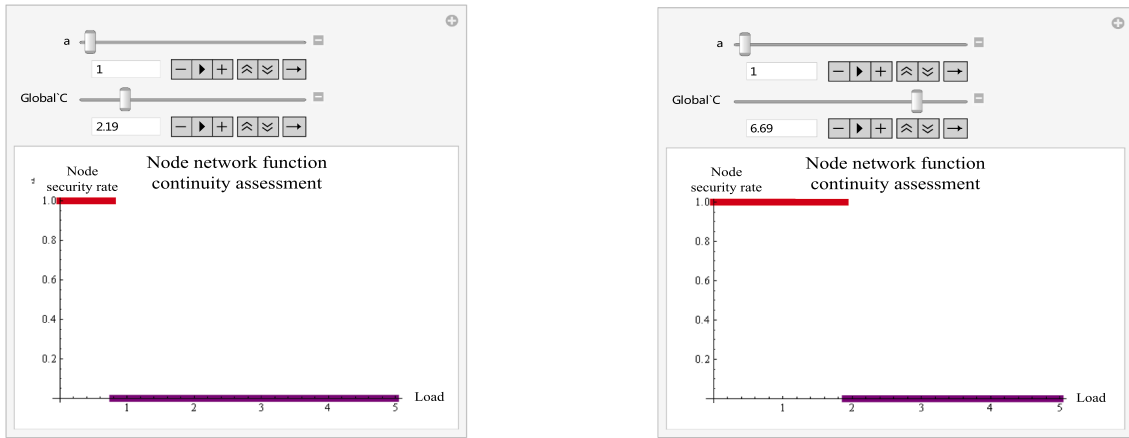


Fig. 8. Node security simulation without considering tolerance.

3.3. Results of navigation station location planning

Take Guiyang airport terminal in China southeast area as an example to analysis the navigation station planning results. According to node business continuity and vulnerability assessment results, Guiyang navigation station is the critical node in the whole network, and it is also the weakness of the network. New navigation station should be built near Guiyang navigation station to weaken the critical effect of Guiyang navigation station in the network. New navigation station is selected from the low efficiency nodes of its adjacent navigation station. It contributes to take full advantage of the navigation stations with redundancy capacity and relief the navigation stations with high node efficiency and high flow load. Besides, new navigation stations should take signal coverage range of Guiyang navigation station as the selected location to satisfy seamless connection among navigation station signals in the whole network. It is shown from Fig. 1, air routes near P_2 , P_1 , P_{14} , P_9 and P_7 are more sparse. Besides, flow loads of these navigation stations are less and some capacity saturations exist in them. Three nodes M_1 , M_2 and M_3 are selected as Fig. 10. New air routes are constructed by connecting new navigation stations with the adjacent navigation stations in original network on the principle of air route non-intersect and navigation station business continuity nonzero. Fig. 11 shows the network topology after adding new navigation stations.

Network business continuity and node efficiency of equipment network will change after adding new navigation stations. After adding each new equipment, network business continuity and node efficiencies of the new equipment network will be calculated for better optimizing

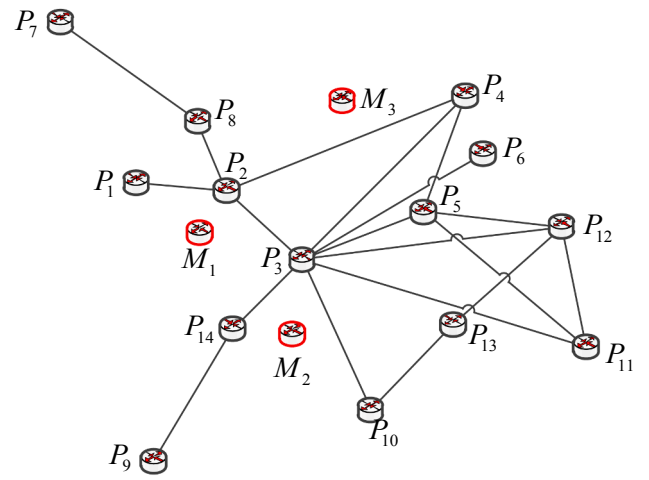


Fig. 10. The selected location of new navigation stations.

location planning, which is displayed in Table 2 regardless of zero edge business continuity.

Table 2 Statistics of air route business continuity and node efficiency in original and new networks

The data in black grids reveal node efficiency of critical node P_3 reduces from 0.79 to 0.77 after adding new navigation station M_3 . By contrast, node efficiency of critical node P_3 increases to 0.81 after

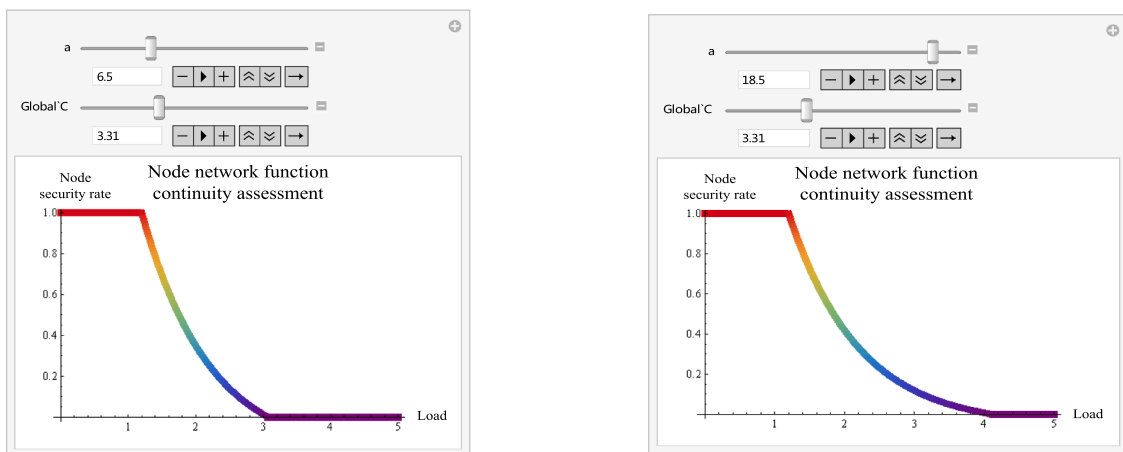


Fig. 9. Node security simulation in the consideration of tolerance.

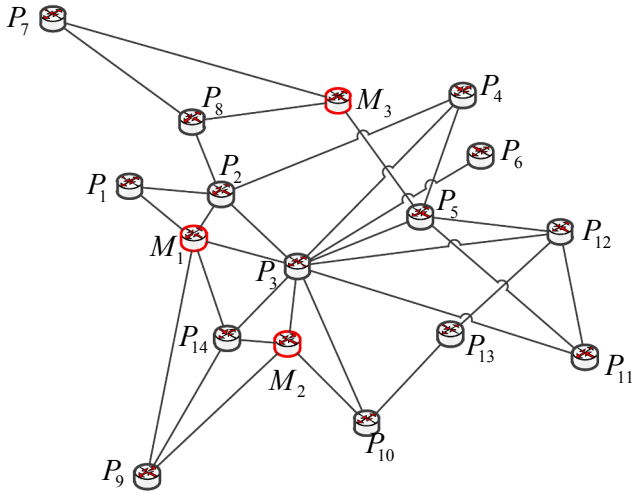


Fig. 11. Network topology after adding new navigation stations.

adding new navigation station M_1 and M_2 . This reflects that the new navigation station M_3 is able to weaken the leading role of critical nodes in network. According to Table 2, the average values and variances of air route business continuity and node efficiencies are obtained, as shown in Table 3.

Table 3 The average values and variances of air route business continuity and node efficiencies

It reveals from Table 3 edge business continuity variance (12.9903) and node efficiency variance (0.018) increase and make the network more sparse after adding new navigation station M_2 compared with those in original network (10.98 and 0.018). Thus, we do not select the navigation station M_2 . But, network nodes and edges are optimized to a certain extent after adding new navigation station M_1 and M_3 . The variance values of them in new network reduce and network security capacity is balanced. The data in Table 3 are taken in to Eq. (18) and Eq. (19).

In the equipment network after adding a new navigation station M_1 .

$$L(M_1) = \begin{Bmatrix} -0.026 \\ 2.068 \end{Bmatrix}, P(M_1) = \begin{Bmatrix} 0.028 \\ 0.007 \end{Bmatrix}$$

In the equipment network after adding a new navigation station M_3 .

$$L(M_3) = \begin{Bmatrix} -0.045 \\ 4.532 \end{Bmatrix}, P(M_3) = \begin{Bmatrix} 0.007 \\ 0.008 \end{Bmatrix}$$

According to the market survey supported by Southwest Regional Air Traffic Management Bureau of Civil Aviation of China, the establishment costs are the costs of navigation station establishment, which is shown in Table 4 are set.

Table 4 Costs of navigation station establishment

The above data are taken into Eq. (25). Then, $M_1 = 3.306$ million, $M_3 = 3.267$ million.

Finally, network business continuity and establishment cost weights are comprehensively considered in this paper. Assuming the period is limited to one year, $k_1 = 1$ million. One million economic consumptions will be brought in the increase of every one unit average business continuity or node efficiency. That is $k_2 = k_1$. 1.5 million economic incomes will be brought in the decrease of every one unit node efficiency variance. That is $k_3 = 1.5k_1$. 0.5 million economic incomes will be brought in the decrease of every one unit edge business continuity variance. That is $k_4 = 0.5k_1$. Then, the following Eq. (30) can be obtained according to Eq. (25).

$$C(M_1) = 2.2845 \text{ million} \quad C(M_3) = 0.951 \text{ million} \quad (30)$$

So, $C(M_1) > C(M_3)$. To sum up, navigation station M_3 is the optimal choice. It not only satisfies the lowest requirement of economic consumption, improves the security and reliability of the whole network, but also reaches optimal network expansion planning.

3.4. Assessment result of network business continuity

New equipment network was constructed with the selected navigation station M_3 . The sustainability assessment of new equipment network was conducted by using the constructed equipment sustainability assessment model in Part 3. By comparing new equipment network with original network, assessment results were shown below.

From the Fig. 14, vulnerability assessment fitting surface of new network is lower than that of original network. This reveals network vulnerability reduces after adding new navigation station. It also means the increases of business continuity. Distances from the highest vulnerability node to other nodes in Fig. 12 are more distant than in

Table 2
Statistics of air route business continuity and node efficiency in original and new networks.

	Original network			New navigation station M_1			New navigation station M_2			New navigation station M_3		
Navig-ation station	Node effici-ency			Air route			Air route betwe-enness			Node effici-ency		
M	None	P8-P2	12	0.65	P8-P2	12	0.60	P8-P2	12	0.53	P2-P3	12
P1	0.41	P8-P4	1	0.48	P8-P4	1	0.40	P8-P4	1	0.40	P2-P4	1
P2	0.63	P8-P3	8	0.67	P8-M1	2	0.62	P8-P3	9	0.62	P2-P8	8
P3	0.79	P8-P14	1	0.81	P8-P3	7	0.81	P8-P14	1	0.77	P2-P10	2
P4	0.52	P8-P12	1	0.57	P8-P12	1	0.57	P8-P12	1	0.57	P2-P12	2
P5	0.60	P8-P10	1	0.59	P8-P10	1	0.59	P8-M2	1	0.63	P2-M3	1
P6	0.48	P2-P4	3	0.47	P2-P4	2	0.45	P2-P4	3	0.46	P3-P5	8
P7	0.34	P2-P3	24	0.34	P2-M1	3	0.33	P2-P3	30	0.42	P3-P8	8
P8	0.46	P2-P14	3	0.47	P2-P3	20	0.56	P2-P12	3	0.51	P3-P10	7
P9	0.37	P2-P12	3	0.45	P2-P12	3	0.43	P2-P10	3	0.36	P3-P12	7
P10	0.52	P2-P10	3	0.52	P2-1P0	3	0.57	P2-M2	3	0.51	P3-M3	4
P11	0.56	P14-P3	11	0.55	M1-P3	13	0.55	P2-P14	3	0.56	P5-P12	4
P12	0.60	P14-P12	1	0.59	M1-P12	2	0.59	P3-P12	7	0.60	P5-M3	11
P13	0.44	P14-P10	1	0.44	M1-P10	2	0.45	P3-P14	10	0.44	P12-M3	2
P14	0.52	P3-P10	8	0.57	P14-P3	7	0.55	P3-M2	9	0.48	P14-P3	12
-	-	P3-P12	8	-	P14-P12	1	-	P3-P10	7	-	P14-P2	3
-	-	-	-	-	P14-10	1	-	P5-P12	1	-	P14-P5	2
-	-	-	-	-	P3-P12	9	-	P10-M2	2	-	P14-P8	1
-	-	-	-	-	P3-P10	9	-	-	-	-	P14-P10	1
-	-	-	-	-	P12-P5	1	-	-	-	-	P14-P12	1
-	-	-	-	-	-	-	-	-	-	-	P14-M3	1
	Total 91 air routes			Total 105 air routes			Total 105 air routes			Total 105 air routes		

Table 3
The average values and variances of air route business continuity and node efficiencies.

	Original network	M_1	M_2	M_3
Edge business continuity average value	0.978	0.95238	1.00952	0.93333
Node efficiency average value	0.517	0.545	0.538	0.524
Edge business continuity variance	10.98	8.91117	12.9903	6.44744
Node efficiency variance	0.018	0.011	0.018	0.0098

Table 4
Costs of navigation station establishment.

Establishment costs (million Yuan)	a	b	c	d	e	f	g	h
M_1	115.6	36	50.4	74	25	4.3	5.3	20
M_3	115.6	35	49.2	78	23	4.2	4.7	17

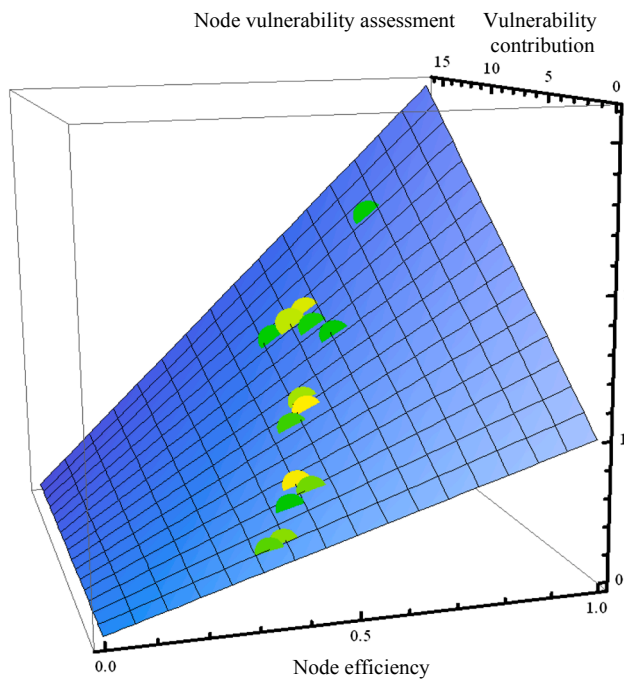


Fig. 12. Node vulnerability assessment result of original network.

Fig. 13. This reveals that the dependence on critical nodes is weakened after adding the new navigation station $-M_3$. The node distribution in **Fig. 13** is more concentrated and uniform than that in **Fig. 12**. This reveals that the node security capacity distribution is more balanced after adding new navigation station $-M_3$.

4. Conclusions

The civil aviation navigation equipment security management support system has been shown helpful to improve the reliability and sustainability of whole civil aviation navigation equipment network. Conclusions of this paper are as follows:

- (1) Use the equipment security weighted network in the support system to figure out a few nodes and edges which carry the lifeblood of the entire network. These nodes and edges, having poor robustness, are the weaknesses in the network and regarded as an alternative area of location planning.
- (2) The decline of node security probability is easing with the increase of navigation station tolerance under the acceptable flow control.

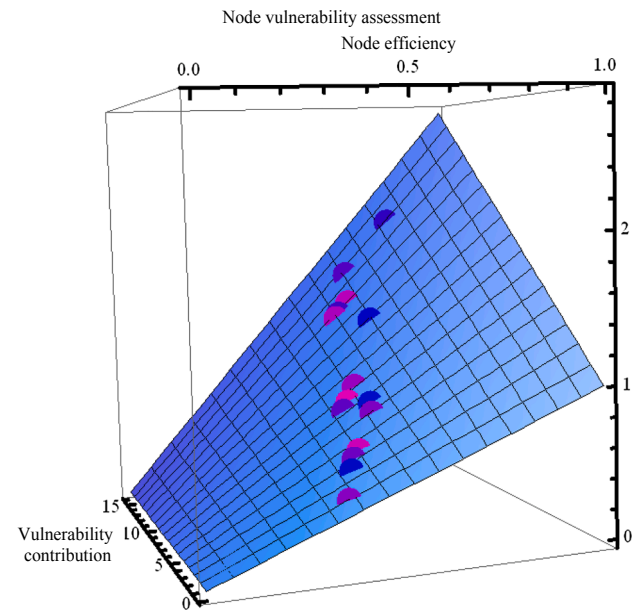


Fig. 13. Node vulnerability assessment result of new network after adding M_3 .

- The increases of each navigation station flow load upper limit mean navigation station capacity saturation virtually increased by some flow control in a constant equipment security capacity.
- (3) After adding each new equipment, network vulnerabilities will reduce and the dependence on critical nodes is weakened, and the node security capacity distribution is more balanced.

This study chose a new viewpoint of network continuity and network vulnerability to search the function of the complex network of aviation security equipment, which can be helpful to the planning of aviation navigation system, and is meaningful to increase the security level of air traffic control management. Concerning the relationship between the security weight and the traffic weight in the civil aviation security equipment network, this paper proposes the concept of equipment security importance, but can only qualitatively measure whether the protection equipment is in its guarantee capability by characterizing the proportional relationship between the protection weight and the traffic weight. To ensure adequate route traffic within the scope, further research is needed to quantitatively calculate the coordinated arrangement between traffic weights and guaranteed weights.

5. Funding

This work is supported by the National Key R&D Program of China (Grant: 2018YFC0809500), the National Natural Science Foundation of China (Grant: 71874081), and the National Natural Science Foundation of China (Grant: 71573122), which provide funds for purchase of software and system construction.

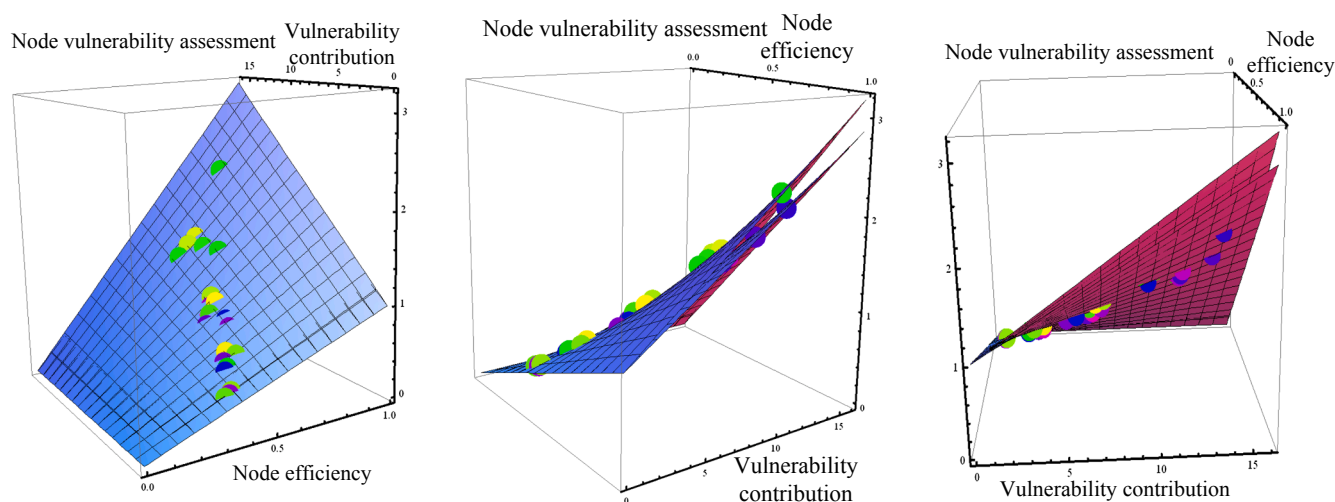


Fig. 14. Comparison of node vulnerability in original and new network.

6. Authors' contributions

SQ contributed to the main idea and designed the system structure. JM designed and carried out the simulation and wrote the code of the simulation program. FX analysed the results. XC participated in results checking and writing. All authors read and approved the final manuscript.

Declaration of Competing Interest

The authors declared that there is no conflict of interest.

References

- Aviation Support Equipment. See website: http://navybm.com/study%20material/14008a/14008A_ch3.pdf.
- Kontogiannis, T., Malakis, S., 2009. A proactive approach to human error detection and identification in aviation and air traffic control. *Saf. Sci.* 47 (5), 693–706. <https://doi.org/10.1016/j.ssci.2008.09.007>.
- Prandini, M., Piroddi, L., Puechmorel, S., Brazdilova, S.L., 2011. Toward air traffic complexity assessment in new generation air traffic management systems. *IEEE Trans. Intell. Transp. Syst.* 12 (3), 809–818. <https://doi.org/10.1109/TITS.2011.2113175>.
- Chen, Fang, Chen, Daogang, Chen, Panfeng, Zheng, Hongyun, 2013. Empirical study of air traffic control safety operation guarantee ability model. *China Safety Sci. J.* 23 (11), 113–119.
- Besada, J., Marquinez, I., Portillo, J., Miguel, G.D., Bernardos, A., 2016. Air traffic generation for new terminal area air traffic management concepts design and evaluation. *Proc. Instit. Mech. Eng. Part G J. Aerospace Eng.* 230 (9), 1721–1732. <https://doi.org/10.1177/0954410015613114>.
- Wang, Yudong, 2014. A novel air traffic management system exploration based on the Internet of things. *Technol. world* 5 (31), 73–74.
- Gravio, G.D., Mancini, M., Patriarca, R., Costantino, F., 2015. Overall safety performance of air traffic management system: forecasting and monitoring. *Saf. Sci.* 72 (22), 351–362. <https://doi.org/10.1016/j.ssci.2014.10.003>.
- Shao, Quan, Kangkang, Wu., Han, Songchen, 2012. Research on facilities layout of air traffic control system based on complex network flow model. *J. Civ. Aviation Univ. China* 30 (6), 29–33.
- Li, Guofa, Zhou, Xingping, Yang, Zhaojun, 2015. The development of toll-pulling force detection device of ATC system for machining centers. *Modular Mach. Tool Automatic Manuf. Tech.* 5, 145–155.
- Feng, Linhan, Yao, Xiongliang, Zhang, Aman, 2010. Vulnerability evaluation of aircraft guarantee system by improved fuzzy petri net. *J. Ship Mech.* 14, 1371–1383.
- Liu, L., Liu, J., Wei, Z., Hui, G., 2016. Transmission line vulnerability assessment based on synergetic effect analysis. *Electric Power Automat. Equip.* 36 (5), 30–37. <https://doi.org/10.16081/j.issn.1006-6047.2016.05.005>.
- Tikhvinskiy, V., Bochechka, G., Korchagin, P., Seilov, S., Gryazev, A., 2017. Sharing spectrum UE LTE and air-traffic control radars in 800 MHz band. *J. Telecommun. Information Technol.* 2, 49.
- Schnell, M., Eppe, U., Shutin, D., Schneckenburger, N., 2014. Ldacs: future aeronautical communications for air-traffic management. *IEEE Commun. Mag.* 52 (5), 104–110.
- Subotic, B., Schuster, W., Majumdar, A., Ochieng, W., 2014. Controller recovery from equipment failures in air traffic control: a framework for the quantitative assessment of the recovery context. *Reliab. Eng. Syst. Saf.* 132, 60–71. <https://doi.org/10.1016/j.res.2014.06.010>.
- Li, Rui, Zhou, Zili, Cheng, Yansong, Wang, Jianqiang, 2017. Failure effects evaluation for ATC automation system. *Appl. Comput. Intell. Soft Comput.* 2017, 1–8. <https://doi.org/10.1155/2017/8304236>.
- Filippov, V.L., Elisov, L.N., Ovchenkov, N.I., 2019. A new approach to the human factor's assessment in the automated control system of aviation security in the airport. *Security Future* 3 (2), 41–42.
- Poghossyan, A., 2018. Provision of basic principles of aviation security in the system of international civil aviation. *Управління безпекою (правосуддя)* 3 (44).
- Li, H., Yang, X., Feng, S., 2019. Design and implementation of international civil aviation security information database management system. *IOP Conf. Series: Earth Environ. Sci. IOP Publ.* 252 (5), 052101.
- Shimizu, Y., Yamazaki, F., Asce, M., Yasuda, S., Towhata, I., Suzuki, T., Isoyama, R., Ishida, E., Suetomi, I., 2006. Development of real-time safety control system for urban gas supply network. *J. Geotech. Geoenviron. Eng.* 132 (2), 237–249. [https://doi.org/10.1061/\(ASCE\)1090-0241\(2006\)132:2\(237\)](https://doi.org/10.1061/(ASCE)1090-0241(2006)132:2(237)).
- Jacob, Rinku, Hari Krishnan, K.P., 2018. Recurrence network measures for hypothesis testing using surrogate data: application to black hole light curves. *Commun. Nonlinear Sci. Numer. Simul.* 54, 84–99. <https://doi.org/10.1016/j.cnsns.2017.05.018>.
- Hejeejo, Rashid, 2017. Probabilistic transmission expansion planning considering distributed generation and demand response programs. *IET Renew. Power Gener.* 11 (5), 650–658. <https://doi.org/10.1049/iet-rpg.2016.0725>.
- Karsten, C.V., Brouer, B.D., Pisinger, D., 2015. Competitive liner shipping network design. *Comput. Oper. Res.* 87, 125–136. <https://doi.org/10.1016/j.cor.2017.05.018>.
- Zhou, Xuan, Zhang, Fengming, Zhou, Weiping, Zou, Wei, Yang, Fan, 2012. Evaluating complex network functional robustness by node efficiency. *Acta Physica Sinica* 61 (19), 1–7. <https://doi.org/10.7498/aps.61.190201>.
- Dai, Fuqing, Wan, Xiaoyan, 2014. Trunk route network planning method based on improved gravity model. *Sci. Technol. Eng.* 14 (3), 1671–1815.